Forest Biomass Retrieval From L-Band SAR Using Tomographic Ground Backscatter Removal

Erik Blomberg, Laurent Ferro-Famil, *Member, IEEE*, Maciej J. Soja, *Member, IEEE*, Lars M. H. Ulander, *Fellow, IEEE*, and Stefano Tebaldini

***Abstract*— A tomographic synthetic aperture radar (TomoSAR) represents a possible route to improved retrievals of forest parameters. Simulated orbital L-band TomoSAR data corresponding to the proposed Satellites for Observation and Communications-Companion Satellite (SAOCOM-CS) mission (1.275 GHz) are evaluated for retrieval of above-ground biomass in boreal forest. L-band data and biomass measurements, collected at the Krycklan test site in northern Sweden as part of the BioSAR 2008 campaign, are used to compare biomass retrievals from SAOCOM-CS to those based on SAOCOM SAR data. Both data sets are in turn compared with the corresponding airborne case, as represented by experimental airborne SAR through processing of the original SAR data. TomoSAR retrievals use a model involving a logarithmic transform of the volumetric backscatter intensity, I_{vol}, defined as the total backscatter originating between 10 and 30 m above ground. SAR retrievals are obtained with slope-compensated intensity γ^0 using the same model. It is concluded that tomography using SAOCOM-CS represents an improvement over an airborne SAR imagery, resulting in biomass retrievals from a single polarization (HH) having a 26%–30% root-mean-square error with a little to no impact from the look direction or the local topography.**

***Index Terms*— Biomass, boreal forest, L-band, Satellites for Observation and Communications-Companion Satellite (SAOCOM-CS), tomography.**

I. Introduction

THE Argentinian Satellites for Observation and Communications (SAOCOM) are a near term earth observation mission consisting of a pair of identical satellites (SAOCOM-1A/1B) and will provide the National Commission for Space Activities of Argentina with L-band synthetic aperture radar (SAR) remote-sensing capabilities. In 2013, the European Space Agency (ESA) was presented with the opportunity to include a passively receiving companion satellite, provisionally designated SAOCOM-Companion Satellite (SAOCOM-CS), on the launch of SAOCOM-1B. The SAOCOM-CS would fly in formation with SAOCOM-1B and permit the acquisition of bistatic, specular, single-pass interferometric, and multipass tomographic L-band SAR data depending on orbital configuration. Basing SAOCOM-CS on the development already performed for SAOCOM and including only the receiving elements aim to lower the technical and economic risks, with work under way to evaluate feasibility and potential scientific return of the proposal [1].

An important potential application is retrieval of above-ground biomass estimates for forests. Forest biomass is a large unknown in current climate modeling, and forest monitoring on a global scale has a large economic and environmental impact. This is reflected in the selection of future earth observation missions and instruments, with BIOMASS and Global Ecosystem Dynamics Investigation (GEDI) being two examples. BIOMASS, a spaceborne P-band SAR, will be ESA's seventh Earth Explorer mission [2], [3] while the GEDI full waveform lidar will be added to the International Space Station as part of NASA's Earth Venture Instruments-2 Program [4]. It can be envisioned that SAOCOM-CS, being an L-band system, would be able to add further observational capabilities and increase both temporal and spatial coverage, especially for those areas of high-latitude boreal forest where observations will be limited for these missions due to spectrum and orbital constraints.

Both airborne and spaceborne L-band SAR systems can provide data for biomass estimation in boreal forests using polarimetric SAR backscatter intensity or interferometric height [5]–[7]. The SAOCOM-CS would provide tomographic profiles as well, which provides information on the vertical scattering distribution. This motivated an evaluation of boreal forest biomass retrieval methods using simulated tomographic SAOCOM-CS data which was part of a 2015 ESA study [8].

It has been shown that tomographic L-band profiles can improve biomass retrievals in temperate forest [9]. This letter is the first to evaluate boreal forest biomass retrieval using L-band tomographic data corresponding to a satellite-based sensor. Tomographic observables are computed from SAOCOM-CS tomograms, simulated by processing airborne L-band SAR images, and used in regression models with *in situ* measurements from a Swedish forestry test site providing training and validation data sets.

II. Experimental Data

All data used for this letter originate from the 2008 BioSAR-2 campaign, which was one of a series of data acquisition campaigns done in support of the future BIOMASS P-band SAR mission [10].

Manuscript received April 20, 2017; revised August 31, 2017 and December 22, 2017; accepted January 15, 2018. This work was supported in part by the Swedish National Space Board under Project 269/14 and Project 164/16 and in part by the European Space Research and Technology Centre, European Space Agency (ESA-ESTEC), under Contract 4000112571/14/NL/FF/gp. *(Corresponding author: Erik Blomberg.)*

E. Blomberg, M. J. Soja, and L. M. H. Ulander are with the Chalmers University of Technology, 412 96 Gothenburg, Sweden (e-mail: erik.blomberg@chalmers.se).

L. Ferro-Famil is with the University of Rennes 1, 35042 Rennes, France.

S. Tebaldini is with the Politecnico di Milano, 20133 Milan, Italy.

Color versions of one or more of the figures in this letter are available online at http://ieeexplore.ieee.org.

Digital Object Identifier 10.1109/LGRS.2018.2819884

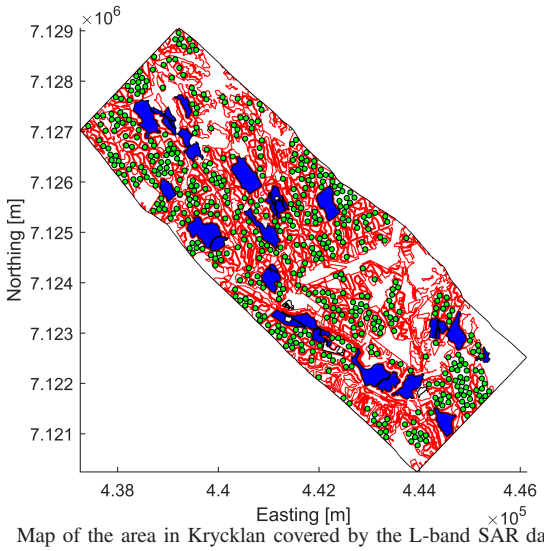

Fig. 1. Map of the area in Krycklan covered by the L-band SAR data used (black outline) and forest stands (red outlines). Circular plots used for training data (green). *In situ* stands used as validation data (blue).

A. BioSAR 2008

BioSAR-2 took place during the late summer and autumn of 2008 and focused on the Krycklan boreal forestry test site. Krycklan is a fairly topographic river catchment located in the north of Sweden (Latitude 64°14′N, Longitude 19°50′E) and contains stands of Norway spruce (*Picea abies*) and Scots pine (*Pinus sylvestris*) in varying proportions with some deciduous elements. The campaign involved extensive field measurements focusing on 31 preselected forest stands of varying shapes and sizes (from 1.5 to 22 ha). Measurements of tree diameter at breast height as well as species, height, and age were taken in circular plots of 10-m radius placed on a regular grid within the stands (about ten plots per stand) [10]. These were used to obtain stand-level estimates for a set of forestry parameters including biomass values with an estimated error of 15% [11].

Coinciding with the forest inventory work was a site covering helicopter-based lidar acquisition on August 5 and 6. These lidar data were processed into digital terrain models and digital canopy models (DCMs) with a 0.5 m × 0.5 m resolution. A 10 m × 10 m forest biomass map was generated from the DCM using *in situ* data from the previously mentioned stands together with an extended set of 110 field plots [10], [12]. A comparison between the *in situ* inventory-based stand estimates of biomass and the corresponding map estimates gives a root-mean-square error (RMSE) of 14 t/ha (16% of the *in situ* stand biomass average of 93 t/ha).

Several sets of P-, L-, and X-band SAR images were acquired on October 14 and 15, 2008 using DLR's experimental airborne SAR (E-SAR) system. This analysis is based on the two sets of L-band images with the largest common coverage: a 3 km by 10 km area running north-west to south-east which covers 26 of the 31 *in situ* stands (see Fig. 1). The two sets correspond to two parallel flight paths, one on a heading of 134° looking in the north-east (NE) direction and one on a heading of 314° looking in the south-west direction. Six horizontally separated baselines were flown for each heading to enable future tomographic processing, resulting in a total of 12 fully polarimetric L-band SAR images [7], [10], [12].

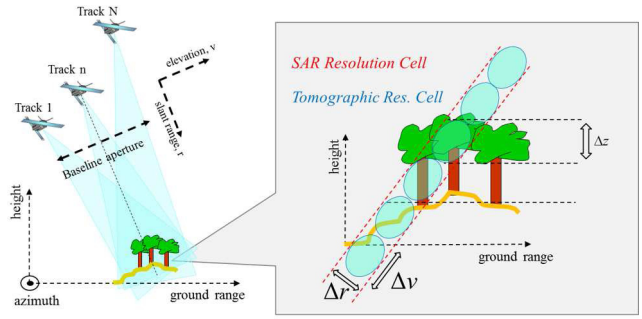

Fig. 2. TomoSAR geometry in the height/ground range plane. The bluish balloons indicate the geometrical extent of the tomographic voxel.

B. Tomographic Processing

A tomographic SAR (TomoSAR) is a microwave imaging technology to focus the illuminated scatterers in the 3-D space, by jointly processing multiple acquisitions from parallel trajectories [13]. The TomoSAR has been used by different research groups in the last years and applied in fields, such as 3-D urban analysis [14], 3-D analysis of snowpack [15], ice [16], [17], glaciers [18], [19], and of course forestry [20]–[22].

In the TomoSAR, multiple flight lines allow the formation of a 2-D synthetic aperture, which allows focusing the signal not only in the range-azimuth plane, as in conventional 2-D SAR imaging, but also in elevation.

A sketch of this concept is shown in Fig. 2, where the SAR resolution cell is split along elevation into several tomographic resolution cells. The geometrical resolution in range and azimuth direction is the same as conventional 2-D SAR, that is $\Delta r = (c/2B)$ and $\Delta x = (\lambda/2L_s)R$, where r and x indicate range and azimuth, respectively, c is the wave velocity in vacuum, B is the pulse bandwidth, λ is the carrier wavelength, L_s is the synthetic aperture length (in azimuth), and R is the stand-off distance from the imaged target. Resolution in elevation follows from the overall baseline aperture: $\Delta v = (\lambda/2b_{\text{ap}})$, where v indicates elevation and b_{ap} is baseline aperture [13]. Vertical resolution is roughly obtained as $\Delta z \simeq \Delta v \cdot \sin\theta$, where θ is the incidence angle [23].

The application of TomoSAR using spaceborne sensors is hindered by the fact that different baselines are usually acquired at time lags on the order of days, limiting the analysis to temporally stable targets (like urban scenarios). A possible mitigation to this potentially limiting scenario is the employment of single pass interferometers, as in the case of Tandem-X (currently operating) and possible future systems, such as Tandem-L and SAOCOM-CS [24], [25].

Such systems achieve the 3-D imaging capabilities by collecting a number of simultaneous interferometric pairs acquired by two satellites, as depicted in Fig. 3. The observed complex coherence corresponds to a particular vertical wavenumber of the imaged scene, depending on the interferometric baseline, i.e., the across-track distance between the two satellites [26]. By collecting multiple pairs with a varying interferometric baseline, it is then possible to obtain multiple vertical wavenumbers, which allows the reconstruction of the vertical distribution of the backscattered power of the imaged scene through spectral-estimation techniques [24], [25].

Table I summarizes the performance requirements for SAOCOM-CS TomoSAR acquisitions over boreal forests.

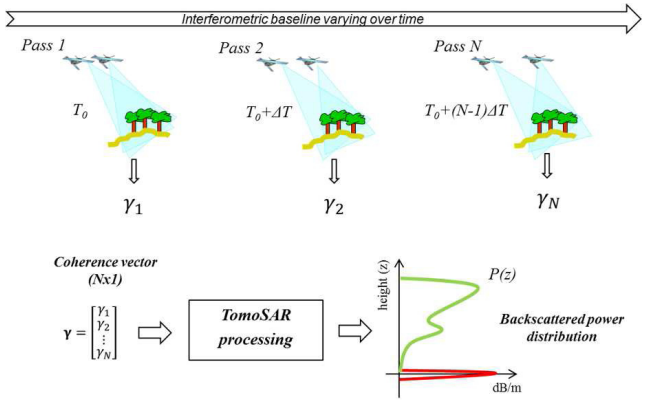

Fig. 3. Tomographic imaging from multiple incoherent passes.

TABLE I
SUMMARY OF SAOCOM-CS TOMOSAR REQUIREMENTS

Metric	Requirement
Number of passes	$N \geq 5$
Height of ambiguity	$z_{amb} \geq 60$ m
Vertical resolution	$dz \leq 20$ m
Spatial SLC resolution	10 m×10 m
Polarization	Dual (Co/Cross-polarized)
Cross-talk	≤ -20 dB

BioSAR-2 data have been processed using a Fourier beamformer and calibrated as described in [27], utilizing both the full 94-MHz E-SAR bandwidth as well as 50 MHz corresponding to the SAOCOM system (by reducing the bandwidth in the frequency domain). The resolution is 1.5 m in slant range by 1 m in azimuth for E-SAR while the nominal ground plane resolution specified for SAOCOM is 10 m by 10 m. The SAOCOM-CS would provide data at 50 m by 50 m with at least 25 looks [8].

At near range, the tomographic configuration of the simulated data is a good match to that envisaged for the SAOCOM-CS, with an identical vertical wavenumber range of 0.1–0.4 m^{-1} and an incidence angle of 25° compared with 23°–27° for the SAOCOM-CS. The results represent a lower limit for the SAOCOM-CS as the data performance decreases in far range, and the resolution was limited equally across the scene. It is worth noting that the near and far range regions are swapped for the two headings. Geocoding errors of the tomographic data were checked using a set of trihedral corner reflectors, with four being visible in each original image, and found to be on the order of the original resolution. Representative examples of each tomographic data set can be seen in Fig. 4.

All SAR backscatter data were obtained from one image per heading, corresponding to a single baseline, using the same parameters and projection as for the tomographic case.

III. METHODOLOGY

A. Observables

γ^0 is a calibrated and slope-compensated intensity parameter [28] and was chosen for the SAR data as it has shown a good sensitivity to biomass and a little dependence on the incidence angle at the L-band [6], [7]. For tomographic evaluation, the parameter chosen is the volumetric backscatter

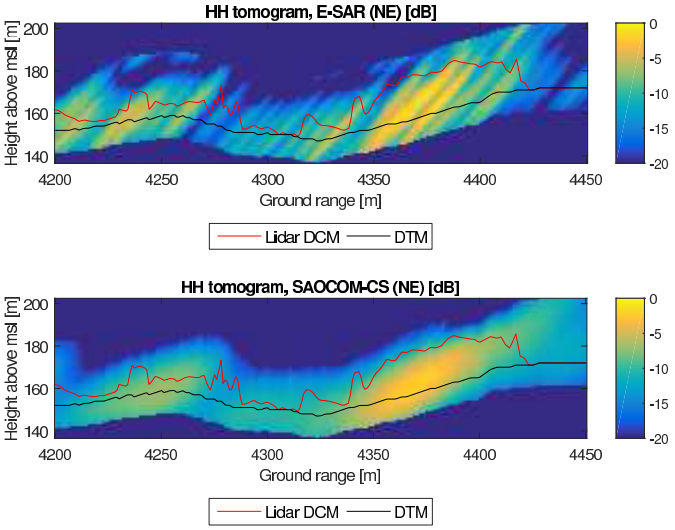

Fig. 4. Example NE-looking HH tomograms for (Top) E-SAR and (Bottom) SAOCOM-CS showing the reduced resolution of the latter. A lidar-derived forest canopy profile (red line) and the local topography (black line) are included for reference.

intensity, $I_{\text{vol}} = \int_{z=10m}^{z=30m} I(z)dz$, i.e., the integrated tomographic backscatter intensity $I(z)$ between 10 and 30 m with z being the vertical height above ground. The energy conserving properties of the Fourier beamformer in combination with the vertical integration result in I_{vol}, retaining the dimensionality and calibration of the original SAR data.

While approaches such as the Legendre basis decomposition of the vertical profile used in [9] can provide more information about forest structure, I_{vol} is intended to minimize the modification of previous backscatter-based models while removing the impact of slope and other effects associated with the ground backscatter. Using 10 m to distinguish between forest volume and ground produced good results in this case, but the thresholds should be reevaluated for other data sets.

B. Retrieval Model

A common approach to the regression analysis is to find a transformation that results in a linear relationship between the variable of interest and the observables, to which a linear model can then be fitted. In this case, a logarithmic transform of biomass and a conversion to decibels proved adept resulting in (1). The model is fitted nonlinearly to obtain a linear error with regard to biomass

$$\hat{B} = \exp\left(a_0 + a_1\left[\gamma^0_{\text{HV}}\right]_{\text{dB}}\right) + \epsilon$$
$$\hat{B} = \exp(a_0 + a_1[I_{\text{vol,HH}}]_{\text{dB}}) + \epsilon. \quad (1)$$

Each model implementation incorporates a single polarization due to the polarimetric components being highly correlated, with Pearson's correlation coefficients of 0.85–0.90 for SAOCOM-CS training data. The best performing polarizations were found to be HV for γ^0 and HH for I_{vol}. The model was used and evaluated for γ^0 at the P-band in [12].

C. Statistical Evaluation

Training data are obtained using a set of virtual forest plots represented by the green circles in Fig. 1. These are 50-m-radius circular plots randomly placed within

TABLE II

FITTING PERFORMANCE STATISTICS FOR THE DIFFERENT PARAMETERS AND MODELS

	Input		RMSE [t/ha]	Bias [t/ha]	R^2	a_0	a_1
γ^0	E-SAR	(NE)	36 (39%)	-19	0.35	38	1.7
		(SW)	33 (36%)	-8	0.34	36	1.5
	SAOCOM	(NE)	36 (39%)	-19	0.34	36	1.5
		(SW)	34 (36%)	-9	0.32	33	1.3
I_{vol}	E-SAR	(NE)	23 (25%)	-8	0.67	4.3	0.21
		(SW)	24 (25%)	-3	0.65	4.5	0.22
	SAOCOM-CS	(NE)	24 (26%)	-11	0.66	9.8	0.71
		(SW)	27 (30%)	-8	0.55	9.7	0.71

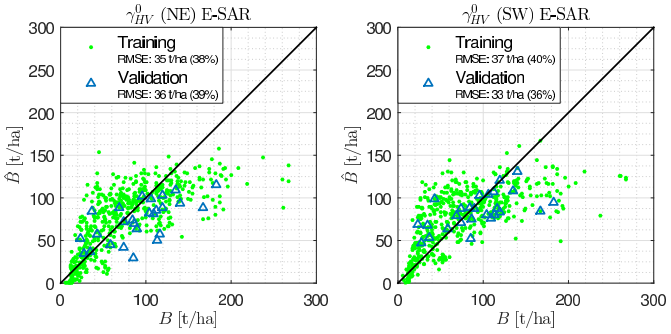

(a)

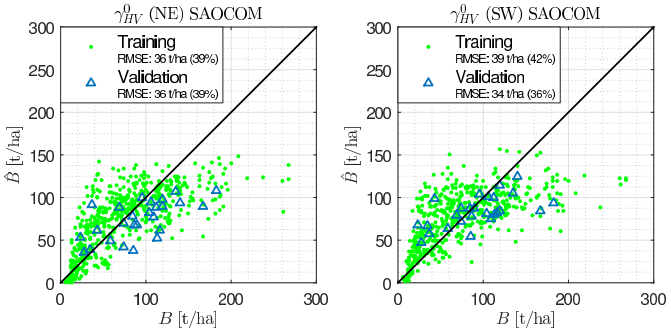

(b)

Fig. 5. Retrievals based on SAR γ^0 HV data for (a) E-SAR and (b) SAOCOM.

homogeneous forest stands while maximizing the area coverage and minimizing the topographic variation within plots. All plot and stand borders are separated by at least 10 m to eliminate spatial overlap of the data. Plot averages of the corresponding data pixels are used as input together with biomass values averaged from the corresponding pixels of the BioSAR-2 biomass map, spanning from 5 to 268 t/ha.

A separate set of 26 stands with *in situ* measurements available is used for validation. These are shown in blue in Fig. 1 and the corresponding data are evaluated at the original resolution before being averaged for each stand. For each retrieval, the coefficient of determination (R^2), RMSE, and bias values are shown in Table II together with the fitted model parameters.

The choice of which data set to use for training and validation is based on having a larger set for regression while reserving the smaller but higher quality set for validation in order to have a high confidence in the reported behavior and

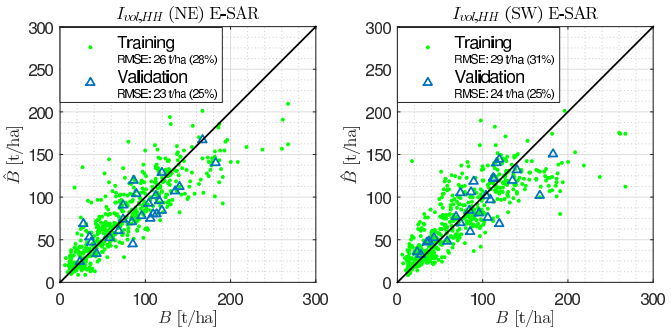

(a)

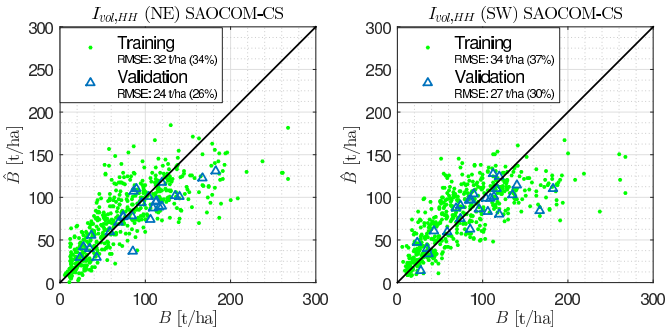

(b)

Fig. 6. Retrievals based on the volumetric HH backscatter, $I_{\mathrm{vol,HH}}$, obtained from tomographic data corresponding to (a) E-SAR and (b) SAOCOM-CS.

evaluation of the errors. The symmetrical shape and constant size of the virtual plots were specifically chosen to facilitate model fitting.

IV. RESULTS

Biomass retrievals obtained using SAR γ^0 intensity data and (1) are shown in Fig. 5, with the results from the high-resolution E-SAR data on top and the reduced bandwidth SAOCOM data on bottom. Similarly, Fig. 6 shows the results obtained for the volumetric backscatter, I_{vol} with the full resolution E-SAR data on top and the simulated SAOCOM-CS data on bottom. The fitted model parameters can be found in Table II.

V. DISCUSSION

As seen from Fig. 5, γ^0 data result in consistent fits with the sizes of the training plots and validation stands being sufficient to negate any impact of the reduced resolution for the SAOCOM. The retrievals indicate some saturation with higher biomass values being underestimated, although the number of validation stands in this range is limited.

The tomographic retrievals shown in Fig. 6 and Table II indicate that I_{vol} is more linearly dependent on biomass, especially for the lowest and highest values. It is clear that biomass retrievals are improved by even the limited suppression of ground level backscatter possible at this vertical resolution. Higher resolution tomography would allow a lower threshold for I_{vol}. E-SAR results are marginally better than the SAOCOM-CS (mostly reflected in the training residuals), which shows the limited impact of the reduced resolution. Of note is also a larger difference between the two headings which is consistent with the variation in vertical resolution across the scene.

Having a good performance using only a single polarization is beneficial from both a technical and operational perspective where acquiring data at multiple polarizations is often traded for coverage or resolution. Improved data might be needed to fully evaluate the performance as the lowest RMSE values obtained are approaching the error of the training and validation data sets. Further incorporating polarimetric and/or phase information is also a possible future improvement.

VI. Conclusion

This letter provided a preliminary assessment of the capability of SAOCOM-CS tomography concerning forest biomass retrieval. The analysis was based on a synthetic data-stack simulated from campaign airborne data. The use of simulated spaceborne data was observed to produce improved biomass retrievals compared with the original airborne intensity data, although not quite as good as the airborne tomographic data. In particular, a parameter obtained from the vertical tomographic intensity profile and the backscatter originating from the forest volume resulted in retrievals with an error of 26%–30% using only HH polarization. Moreover, these results were obtained using 50-m plots, which suggest further improvement by aggregating the data at a larger scale.

It is important to remark that a comprehensive assessment of the capability of SAOCOM-CS concerning biomass retrieval would include not only the elements that we considered in this letter, such as spatial resolution and geometrical baselines, but also others, such as system noise, ambiguities, and bistatic synchronization. Also forest type is indeed to be considered. Still, we deem that the results of this letter are encouraging regarding the applicability of the SAOCOM-CS tomography for forest biomass retrieval. Future research will be focused on performance assessment with more realistic simulations as well as on extending the investigation to different forest sites.

Acknowledgment

The authors would like to thank the Department of Forest Resource Management at the Swedish University of Agricultural Sciences for field data collection and processing of forestry and lidar products as well as the European Space Agency with contributors for the BioSAR 2008 data set.

References

[1] N. Gebert, B. C. Dominguez, M. W. J. Davidson, M. D. Martin, and P. Silvestrin, "SAOCOM-CS—A passive companion to SAOCOM for single-pass L-band SAR interferometry," in *Proc. EUSAR*, Berlin, Germany, Jun. 2014, pp. 1251–1254.

[2] T. Le Toan *et al.*, "The BIOMASS mission: Mapping global forest biomass to better understand the terrestrial carbon cycle," *Remote Sens. Environ.*, vol. 115, no. 11, pp. 2850–2860, Nov. 2011.

[3] F. Heliere, F. Fois, M. Arcioni, P. Bensi, M. Fehringer, and K. Scipal, "Biomass P-band SAR interferometric mission selected as 7th Earth Explorer Mission," in *Proc. EUSAR*, Berlin, Germany, Jun. 2014, pp. 1152–1155.

[4] NASA Science Missions. *Global Ecosystem Dynamics Investigation Lidar*. Accessed: Mar. 14, 2017. [Online]. Available: https://science.nasa.gov/missions/gedi

[5] M. Santoro, J. E. S. Fransson, L. E. B. Eriksson, M. Magnusson, L. M. H. Ulander, and H. Olsson, "Signatures of ALOS PALSAR L-band backscatter in swedish forest," *IEEE Trans. Geosci. Remote Sens.*, vol. 47, no. 12, pp. 4001–4019, Dec. 2009.

[6] G. Sandberg, L. M. H. Ulander, J. E. S. Fransson, J. Holmgren, and T. Le Toan, "L- and P-band backscatter intensity for biomass retrieval in hemiboreal forest," *Remote Sens. Environ.*, vol. 115, no. 11, pp. 2874–2886, Nov. 2011.

[7] M. Neumann, S. S. Saatchi, L. M. H. Ulander, and J. E. S. Fransson, "Assessing performance of L- and P-band polarimetric interferometric SAR data in estimating boreal forest above-ground biomass," *IEEE Trans. Geosci. Remote Sens.*, vol. 50, no. 3, pp. 714–726, Mar. 2012.

[8] S. Tebaldini *et al.*, "Study of L- and P-band SAR tomography synergies," ESA-ESTEC, Noordwijk, The Netherlands, Tech. Rep. 4000112571/14/NL/FF/gp, 2015.

[9] A. T. Caicoya, M. Pardini, I. Hajnsek, and K. Papathanassiou, "Forest above-ground biomass estimation from vertical reflectivity profiles at L-band," *IEEE Geosci. Remote Sens. Lett.*, vol. 12, no. 12, pp. 2379–2383, Dec. 2015.

[10] I. Hajnsek *et al.*, "BIOSAR 2008: Final report," ESA-ESTEC, Noordwijk, The Netherlands, Tech. Rep. 22052/08/NL/CT-002, 2009.

[11] M. J. Soja, H. J. Persson, and L. M. H. Ulander, "Estimation of forest biomass from two-level model inversion of single-pass InSAR data," *IEEE Trans. Geosci. Remote Sens.*, vol. 53, no. 9, pp. 5083–5099, Sep. 2015.

[12] M. J. Soja, G. Sandberg, and L. M. H. Ulander, "Regression-based retrieval of boreal forest biomass in sloping terrain using P-band SAR backscatter intensity data," *IEEE Trans. Geosci. Remote Sens.*, vol. 51, no. 5, pp. 2646–2665, May 2013.

[13] A. Reigber and A. Moreira, "First demonstration of airborne SAR tomography using multibaseline L-band data," *IEEE Trans. Geosci. Remote Sens.*, vol. 38, no. 5, pp. 2142–2152, Sep. 2000.

[14] X. X. Zhu and R. Bamler, "Very high resolution spaceborne SAR tomography in urban environment," *IEEE Trans. Geosci. Remote Sens.*, vol. 48, no. 12, pp. 4296–4308, Dec. 2010.

[15] L. Ferro-Famil, S. Tebaldini, M. Davy, and F. Boute, "3D SAR imaging of the snowpack in presence of propagation velocity changes: Results from the AlpSAR campaign," in *Proc. IEEE Int. Geosci. Remote Sens. Symp.*, Quebec City, QC, Canada, Jul. 2014, pp. 3370–3373.

[16] F. Banda, J. Dall, and S. Tebaldini, "Single and multipolarimetric P-band SAR tomography of subsurface ice structure," *IEEE Trans. Geosci. Remote Sens.*, vol. 54, no. 5, pp. 2832–2845, May 2016.

[17] T. G. Yitayew, L. Ferro-famil, T. Eltoft, and S. Tebaldini, "Tomographic imaging of Fjord ice using a very high resolution ground-based SAR system," *IEEE Trans. Geosci. Remote Sens.*, vol. 55, no. 2, pp. 698–714, Feb. 2017.

[18] O. Ponce, P. Prats, R. Scheiber, A. Reigber, I. Hajnsek, and A. Moreira, "Polarimetric 3-D imaging with airborne holographic SAR tomography over glaciers," in *Proc. IEEE Int. Geosci. Remote Sens. Symp.*, Milan, Italy, Jul. 2015, pp. 5280–5283.

[19] S. Tebaldini, T. Nagler, H. Rott, and A. Heilig, "L-band 3D imaging of an alpine glacier: Results from the AlpTomoSAR campaign," in *Proc. IEEE Int. Geosci. Remote Sens. Symp.*, Milan, Italy, Jul. 2015, pp. 5212–5215.

[20] S. Tebaldini and F. Rocca, "Multibaseline polarimetric SAR tomography of a boreal forest at P- and L-bands," *IEEE Trans. Geosci. Remote Sens.*, vol. 50, no. 1, pp. 232–246, Jan. 2012.

[21] O. Frey and E. Meier, "Analyzing tomographic SAR data of a forest with respect to frequency, polarization, and focusing technique," *IEEE Trans. Geosci. Remote Sens.*, vol. 49, no. 10, pp. 3648–3659, Oct. 2011.

[22] D. H. T. Minh, T. Le Toan, F. Rocca, S. Tebaldini, M. M. D'Alessandro, and L. Villard, "Relating P-band synthetic aperture radar tomography to tropical forest biomass," *IEEE Trans. Geosci. Remote Sens.*, vol. 52, no. 2, pp. 967–979, Feb. 2014.

[23] S. Tebaldini, "Single and multipolarimetric SAR tomography of forested areas: A parametric approach," *IEEE Trans. Geosci. Remote Sens.*, vol. 48, no. 5, pp. 2375–2387, May 2010.

[24] A. Moreira *et al.*, "Tandem-L: A highly innovative bistatic SAR mission for global observation of dynamic processes on the Earth's surface," *IEEE Geosci. Remote Sens. Mag.*, vol. 3, no. 2, pp. 8–23, Jun. 2015.

[25] *SAOCOM Companion Satellite Science Report*, document EOP-SM/2764/MWJD-mwjd, ESA-ESTEC, Noordwijk, The Netherlands, 2015.

[26] R. Bamler and P. Hartl, "Synthetic aperture radar interferometry," *Inverse Problems*, vol. 14, no. 4, pp. R1–R54, Aug. 1998.

[27] S. Tebaldini, F. Rocca, M. M. D'Alessandro, and L. Ferro-Famil, "Phase calibration of airborne tomographic sar data via phase center double localization," *IEEE Trans. Geosci. Remote Sens.*, vol. 54, no. 3, pp. 1775–1792, Mar. 2016.

[28] L. M. H. Ulander, "Radiometric slope correction of synthetic-aperture radar images," *IEEE Trans. Geosci. Remote Sens.*, vol. 34, no. 5, pp. 1115–1122, Sep. 1996.